Substituent Effects on the Energies of the Electronic Transitions of Geminally Diphenyl-Substituted Trimethylenemethane (TMM) Radical Cations. Experimental and Theoretical Evidence for a Twisted Molecular and Localized Electronic Structure

Hayato Namai,[†] Hiroshi Ikeda,*[,‡] Nobuyuki Kato,[†] and Kazuhiko Mizuno[‡]

Department of Chemistry, Graduate School of Science, Tohoku University, Sendai 980-8578, Japan, and Department of Applied Chemistry, Graduate School of Engineering, Osaka Prefecture University, Sakai, Osaka 599-8531, Japan

Received: December 4, 2006; In Final Form: February 6, 2007

Substituent effects on the energies (E_{ob}) of electronic transitions of geminally diphenyl-substituted trimethylenemethane (TMM) radical cations **5a**−**k**$^{\bullet+}$ and those of structurally related 1,1-diarylethyl cations **7a**−**k**$^{+}$ were determined experimentally by using electronic transition spectroscopy. In addition, transition energies of these radical cations were determined by using density functional theory (DFT) and time-dependent (TD)-DFT calculations. The electronic transition bands of **5a**−**k**$^{\bullet+}$ and **7a**−**k**$^{+}$ have maxima (λ_{ob}) that appear at 500−432 and 472−422 nm, respectively. A Hammett treatment made by plotting the E_{ob} values relative to that of the diphenyl-TMM radical cation **5d**$^{\bullet+}$ (ΔE_{ob}) vs the cationic substituent parameter σ^{+} give a favorable correlation with a boundary point at $\sigma^{+} = 0.00$ and a positive ρ for $\sigma^{+} < 0$ and a negative ρ for $\sigma^{+} > 0$. A comparison of the λ_{ob} and ρ values for **5a**−**k**$^{\bullet+}$ and **7a**−**k**$^{+}$ suggests that the chromophore of **5**$^{\bullet+}$ is substantially the same as that of **7**$^{+}$. The results of TD-DFT calculations, which reproduce the experimental electronic transition spectra and relationships between ΔE_{ob} and σ^{+}, and suggest that the absorption band of **5**$^{\bullet+}$ is associated with the SOMO−X → SOMO transition, while that of **7**$^{+}$ is due to the HOMO → LUMO transition. Another interesting observation is that Cl and Br substituents in the diphenyl-substituted TMM radical cations and 1,1-diarylethyl cations **7a**−**k**$^{+}$ act as electron-donating groups in terms of their effect on the corresponding electronic transitions. The results show that the molecular structure of **5**$^{\bullet+}$ is a considerably twisted and that **5**$^{\bullet+}$ has a substantially localized electronic state in which the positive charge and odd electron are localized in the respective diarylmethyl and the allyl moieties.

Introduction

The trimethylenemethane (TMM, **1**$^{\bullet\bullet}$ in Chart 1) biradical and its derivatives have been a target of many theoretical and experimental investigations since Moffitt[1] first predicted its unique electronic structure and Dowd[2] observed it spectroscopically by using ESR. In recent years, the high reactivity and large paramagnetism of this biradical have attracted much attention from scientists in the areas of organic synthesis,[3] DNA cleaving reagents,[4] and molecular-based magnetic materials.[5] Particular emphasis has been given to aryl-substituted trimethylenemethane biradicals[6] owing to their ease of preparation, handling, and chemical modification.

Questions about the molecular and electronic structures of substituted TMMs,[7] especially derivatives possessing aryl substitution,[6,8,9] led us to further embark on an investigation of these systems. By using absorption and emission spectroscopy and density functional theory (DFT) calculations on the diphenyl-substituted TMM biradical (Berson's TMM, **3**$^{\bullet\bullet}$, Scheme 1),[8,9] generated in a low-temperature matrix by photoinduced deazetation of 7-(diphenylmethylene)-2,3-diazabicyclo-[2.2.1]hept-2-ene (**2**), we showed that the ground state species has a nearly planar conformation ($\theta = 23.5°$) and a highly localized electronic state. Also, the results of our studies[10] of photoinduced electron-transfer (PET) reactions of 2,2-diphenyl- and 2,2-bis(4-methoxyphenyl)-1-methylenecyclopropanes (**4d** and **4a**, Scheme 2) demonstrated that the TMM radical cations (**5**$^{\bullet+}$) and the TMM biradicals (**5**$^{\bullet\bullet}$) are intermediates in the ensuing reaction pathways. Interestingly, calculations suggest that the molecular geometries of **5**$^{\bullet+}$ and **5**$^{\bullet\bullet}$ are twisted ($\theta = 44°$ [10a] for **5a**$^{\bullet+}$ by AM1 UHF, $\theta = 44°$ [11] for **5d**$^{\bullet+}$ by UB3LYP/

CHART 1: Parent TMM (1$^{\bullet\bullet}$*) and Its Radical Cation (1$^{\bullet+}$)

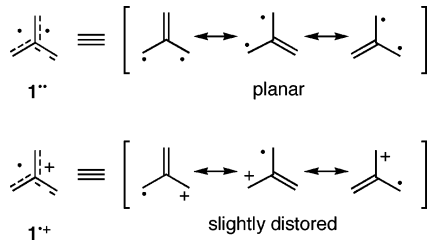

SCHEME 1: Generation of Berson's TMM (3$^{\bullet\bullet}$)[a]

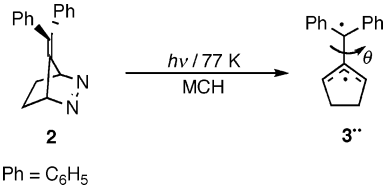

[a] Abbreviation: MCH, methylcyclohexane.

* To whom correspondence should be addressed. E-mail: ikeda@chem.osakafu-u.ac.jp.
[†] Tohoku University (TU).
[‡] Osaka Prefecture University.

10.1021/jp068308l CCC: $37.00
Published on Web 05/02/2007

SCHEME 2: Mechanism for the PET MCP Rearrangement of 4[a]

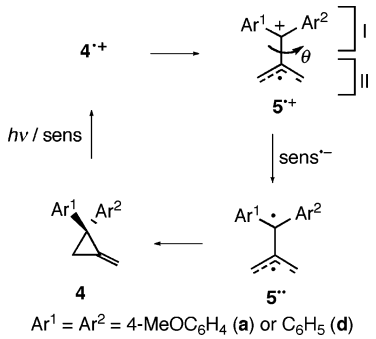

[a] Abbreviation: sens, sensitizer.

SCHEME 3: Plausible Mechanism for the Thermoluminescence (TL) of 5d••*

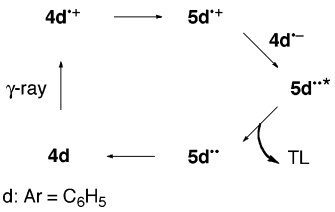

cc-pVDZ and $\theta = 32.3°$[12] for **5d••** by UB3LYP/cc-pVDZ) and that the electronic states of these transients are comprised of a diarylmethyl cation moiety (or radical, subunit I, Scheme 2) and an allyl radical moiety (subunit II). Moreover, we discovered that the radical cation **5d**$^{\bullet+}$ is a key precursor of the excited TMM biradical **5d**••* formed in this process and that **5d**••* shows intense thermoluminescence (Scheme 3) in a methylcyclohexane (MCH) matrix at ca. 130 K after γ-irradiation.[13]

Gaining detailed knowledge about the molecular and electronic structures of trimethylenemethane radical cations **5**$^{\bullet+}$ is a significant undertaking owing to the relationships that exist between (1) its structural and electronic features and the efficiencies of its transformations to **5d••** and **5d••*** as well as (2) the corresponding radical anion **5d**$^{\bullet-}$.[14] In addition, it is important to know about how substitution on the phenyl rings of the parent TMM radical cation (**1**$^{\bullet+}$, Chart 1), reported to be slightly distorted by a static Jahn−Teller effect,[15] influence its molecular structure. Studying substituent effects on the energies (E) of electronic transitions is a useful way to probe the molecular and electronic structures of **5**$^{\bullet+}$. Therefore, we determined E for members of a series of diaryl TMM radical cations **5a**−**k**$^{\bullet+}$, generated by γ-irradiation of *n*-butyl chloride (*n*-BuCl) matrices containing the methylenecyclopropanes **4a**−**k** at 77 K (Scheme 4). For comparison, the transition energies of 1,1-diarylethyl cations (**7a**−**k**$^{+}$), generated from the corresponding alcohols (**6a**−**k**) in fluorosulfonic acid (FSO_3H) at 196 K (Scheme 4), were also determined. To gain further insight into these spectroscopic properties, DFT and time-dependent (TD)-DFT calculations were performed on **5a**−**f**$^{\bullet+}$ and **7a**−**f**$^{+}$. Below, we describe the results of this combined experimental and theoretical effort, which demonstrate that the molecular structure of **5**$^{\bullet+}$ is considerably twisted and that its electronic structure is highly localized.

Experimental Section

General Method. See the Supporting Information.

Preparation of 2,2-Diaryl-1-methylenecyclopropanes 4 and 1,1-Diarylethanols 6. 2,2-Diaryl-1-methylenecyclopropanes **4** were prepared from the corresponding 1,1-diarylethylenes **10** via 2,2-diaryl-1,1-dibromocyclopropanes **11** and 2,2-diaryl-1-bromo-1-methylcyclopropanes **12** according to the procedure reported for the preparation of **4a** (Scheme 5).[10a] Diarylethylenes **10** were obtained by using Wittig reactions of benzophenone derivatives **8** or by dehydration of 1,1-diarylethanols **6**, which were obtained by using the Grignard reactions of **8** or acetophenone derivatives **9**. See the Supporting Information for physical data of key compounds.

SCHEME 4: Generation of 5$^{\bullet+}$ **and 7**$^{+}$[a]

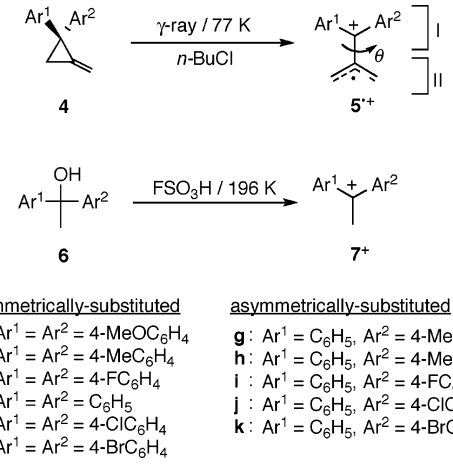

[a] Abbreviation: *n*-BuCl, *n*-butyl chloride.

SCHEME 5: Outline of the Synthesis of 4[a]

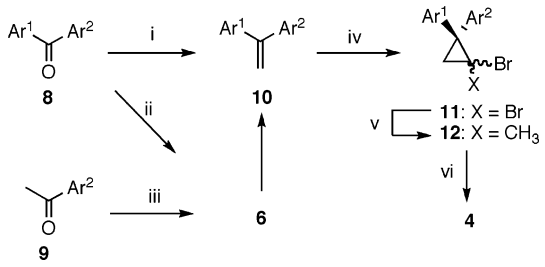

[a] Reagents and conditions: (i) PPh_3CH_3Br, *t*-BuOK, THF; (ii) CH_3I, Mg, diethyl ether or *n*-BuLi, diethyl ether; (iii) Ar^1Br, Mg, THF; (iv) $CHBr_3$, NaOH aq, $PhCH_2Et_3NCl$; (v) CH_3I, *n*-BuLi, THF; (vi) *t*-BuOK, DMSO.

Electronic Absorption Spectra of 5$^{\bullet+}$**.** An *n*-BuCl solution (1 mL) containing **4** (5 mM) in a flat vessel (synthetic quartz, $2 \times 10 \times 40$ mm^3 thickness × width × height) was degassed by five freeze (77 K)−pump (10^{-3} Torr)−thaw (ambient temperature) cycles and then sealed at 10^{-2} Torr. The glassy matrix, obtained by steeping the vessel into liquid nitrogen, was irradiated with γ-rays from a 5.1 TBq ^{60}Co source in liquid nitrogen at 77 K for 40 h. The absorption spectra were recorded at 77 K before and after irradiation.

Electronic Absorption Spectra of 7^{+}**.** A methanol solution of the alcohol **6** (1 mM) was added dropwise in 20 μL portions to 2 mL FSO_3H in a flat vessel (quartz, $10 \times 10 \times 40$ mm^3 thickness × width × height) cooled at 196 K. The absorption spectra at 196 K were recorded while the solution was added.

Quantum Chemical Calculations. Geometry optimization was performed with the cc-pVDZ basis set by using Becke's hybrid, three-parameter functional[16] and the nonlocal correlation functional of Lee, Yang, and Parr (B3LYP).[17] Excitation energies were computed using time-dependent density functional theory (TD-B3LYP) with the cc-pVDZ basis set. All of the

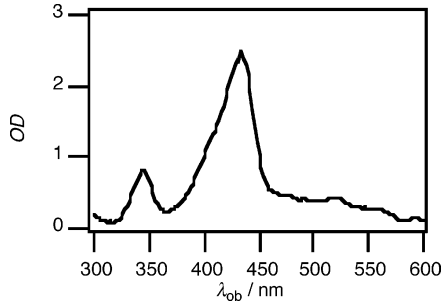

Figure 1. Electronic absorption spectra of $\mathbf{5d}^{\bullet+}$ observed after γ-irradiation of **4d** (5 mM) in *n*-BuCl glassy matrix at 77 K.

TABLE 1: Observed and Calculated[a] Electronic Absorption Maxima (λ_{ob} and λ_{cal}), Relative Energies (ΔE_{ob} and ΔE_{cal}), and Oscillator Strengths (f) of 5a−k$^{\bullet+}$

species	λ_{ob}/nm	ΔE_{ob}/kcal mol^{-1}	λ_{cal}/nm	f	ΔE_{cal}/kcal mol^{-1}
5a$^{\bullet+}$	500	−9.00	426	0.68	−8.91
5b$^{\bullet+}$	460	−4.03	399	0.62	−4.39
5c$^{\bullet+}$	438	−0.91	387	0.51	−2.19
5d$^{\bullet+}$	432	0.00	376	0.44	0.00
5e$^{\bullet+}$	462	−4.30	425	0.67	−8.66
5f$^{\bullet+}$	478	−6.37	453	0.70	−12.90
5g$^{\bullet+}$	466	−4.83	*b*		
5h$^{\bullet+}$	448	−2.36	*b*		
5i$^{\bullet+}$	434	−0.30	*b*		
5j$^{\bullet+}$	450	−2.65	*b*		
5k$^{\bullet+}$	456	−3.48	*b*		

[a] Calculations were carried out with TD-UB3LYP/cc-pVDZ. [b] No attempt.

calculations were performed with the program Gaussian 98.[18] Figures 4−6 were drawn using WinMOPAC 3.9 software.[19]

Results

Electronic Absorption Spectra of 5$^{\bullet+}$ and 7$^+$. γ-Irradiation of *n*-BuCl glassy matrices containing **4a**−**k** at 77 K led to the production of sharp electronic absorption bands with λ_{ob} at 500, 460, 438, 432, 462, 478, 466, 448, 434, 450, and 456 nm, respectively (Figure 1, Table 1). The absorption bands were assigned to electronic transitions of the TMM radical cations $\mathbf{5a}-\mathbf{k}^{\bullet+}$, respectively.[11] The differences in the observed electronic transition energies (E_{ob}) of $\mathbf{5a}-\mathbf{k}^{\bullet+}$ relative to the E_{ob} of $\mathbf{5d}^{\bullet+}$ (ΔE_{ob}) were found to be −9.00, −4.03, −0.91, 0.00, −4.30, −6.37, −4.83, −2.36, −0.30, −2.65, and −3.48 kcal mol^{-1}, respectively (Table 1).

For comparison purposes, electronic absorption spectra of diarylethyl cations $\mathbf{7a}-\mathbf{k}^+$, formed by dissolving diarylethyl alcohols **6a**−**k** in FSO_3H at 196 K, were measured. In a manner analogous to $\mathbf{5a}-\mathbf{k}^{\bullet+}$, $\mathbf{7a}-\mathbf{k}^+$ have intense, sharp absorption bands with λ_{ob} at 472, 450, 430, 422, 458, 470, 442, 436, 426, 442, and 448 nm, respectively (Figure 2 and Table 2). The ΔE_{ob} of $\mathbf{7a}-\mathbf{k}^+$ relative to $\mathbf{7d}^+$ were calculated to be −7.17, −4.21, −1.26, 0.00, −5.32, −6.92, −3.06, −2.17, −0.64, −3.06, and −3.93 kcal mol^{-1}, respectively (Table 2).

Hammett Plots of ΔE vs σ^+ for 5a−k$^{\bullet+}$ and 7a−k$^+$. To gain insight into the origin of the effects of substituents in $\mathbf{5a}-\mathbf{k}^{\bullet+}$ and $\mathbf{7a}-\mathbf{k}^+$ on E_{ob}, Hammett plots of ΔE_{ob} vs σ^+ (−0.78, −0.31, −0.07, 0.00, +0.11, and +0.15 for MeO, Me, F, H, Cl, and Br groups, respectively) were constructed (Figure 3a−d). The plots show that two linear correlations exist for the data obtained from $\mathbf{5a}-\mathbf{k}^{\bullet+}$ and $\mathbf{7a}-\mathbf{k}^+$. The lines obtained have respective positive and negative slopes with the boundary point at $\sigma^+ = 0.00$. The Hammett plot correlations for $\mathbf{5a}-\mathbf{f}^{\bullet+}$, $\mathbf{7a}-\mathbf{f}^+$, $\mathbf{5g}-\mathbf{k}^{\bullet+}$, and $\mathbf{7g}-\mathbf{k}^+$ (Figure 3a−d) are given in eqs 1−8,

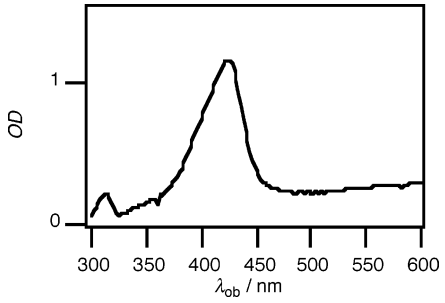

Figure 2. Electronic absorption spectra of $\mathbf{7d}^+$ generated from **6d** in FSO_3H at 196 K.

TABLE 2: Observed and Calculated[a] Electronic Absorption Maxima (λ_{ob} and λ_{cal}), Relative Energies (ΔE_{ob} and ΔE_{cal}), and Oscillator Strengths (f) of 7a−k$^+$

species	λ_{ob}/nm	ΔE_{ob}/kcal mol^{-1}	λ_{cal}/nm	f	ΔE_{cal}/kcal mol^{-1}
7a$^+$	472	−7.17	423	0.77	−8.69
7b$^+$	450	−4.21	398	0.70	−4.42
7c$^+$	430	−1.26	387	0.33	−2.40
7d$^+$	422	0.00	375	0.52	0.00
7e$^+$	458	−5.32	424	0.76	−8.80
7f$^+$	470	−6.92	452	0.79	−13.0
7g$^+$	442	−3.06	*b*		
7h$^+$	436	−2.17	*b*		
7i$^+$	426	−0.64	*b*		
7j$^+$	442	−3.06	*b*		
7k$^+$	448	−3.93	*b*		

[a] Calculations were carried out with TD-B3LYP/cc-pVDZ. [b] No attempt.

respectively. Plots of the data from the symmetrically substituted TMM radical cations ($\mathbf{5a}-\mathbf{f}^{\bullet+}$) and diarylethyl cations ($\mathbf{7a}-\mathbf{f}^+$) give respective slopes of +11.5 and +13.2 for $\sigma^+ < 0$ and of −41.7 and −46.6 for $\sigma^+ > 0$. Similarly, plots for the asymmetrically substituted TMM radical cations ($\mathbf{5g}-\mathbf{k}^{\bullet+}$) and diarylethyl cations ($\mathbf{7g}-\mathbf{k}^+$) give slopes of +6.29 and +6.84 for $\sigma^+ < 0$ and of −23.4 and −26.5 for $\sigma^+ > 0$, respectively. Here, we define the slopes in regions $\sigma^+ < 0$ and $\sigma^+ > 0$ as ρ and ρ', respectively, based on the Hammett relationship.

$$\sigma^+ < 0$$

$$\Delta E_{ob} = 11.5\sigma^+ - 0.15 \quad \text{for } \mathbf{5a}-\mathbf{f}^{\bullet+} \tag{1}$$

$$\Delta E_{ob} = 13.2\sigma^+ - 0.15 \quad \text{for } \mathbf{7a}-\mathbf{f}^{+}\ ^{20} \tag{2}$$

$$\Delta E_{ob} = 6.29\sigma^+ - 0.05 \quad \text{for } \mathbf{5g}-\mathbf{k}^{\bullet+} \tag{3}$$

$$\Delta E_{ob} = 6.84\sigma^+ - 0.07 \quad \text{for } \mathbf{7g}-\mathbf{k}^{+}\ ^{20} \tag{4}$$

$$\sigma^+ > 0$$

$$\Delta E_{ob} = -41.7\sigma^+ - 0.06 \quad \text{for } \mathbf{5a}-\mathbf{f}^{\bullet+} \tag{5}$$

$$\Delta E_{ob} = -46.6\sigma^+ - 0.04 \quad \text{for } \mathbf{7a}-\mathbf{f}^{+} \tag{6}$$

$$\Delta E_{ob} = -23.4\sigma^+ - 0.02 \quad \text{for } \mathbf{5g}-\mathbf{k}^{\bullet+} \tag{7}$$

$$\Delta E_{ob} = -26.5\sigma^+ - 0.03 \quad \text{for } \mathbf{7g}-\mathbf{k}^{+} \tag{8}$$

Discussion

Substituent Effects on the Electronic Transition Energies of 5a−k$^{\bullet+}$ and 7a−k$^+$. Information about the structural and electronic properties of TMM radical cations has come from a comparison of substituent effects on the energies for electronic transitions in the symmetrically substituted radical cations

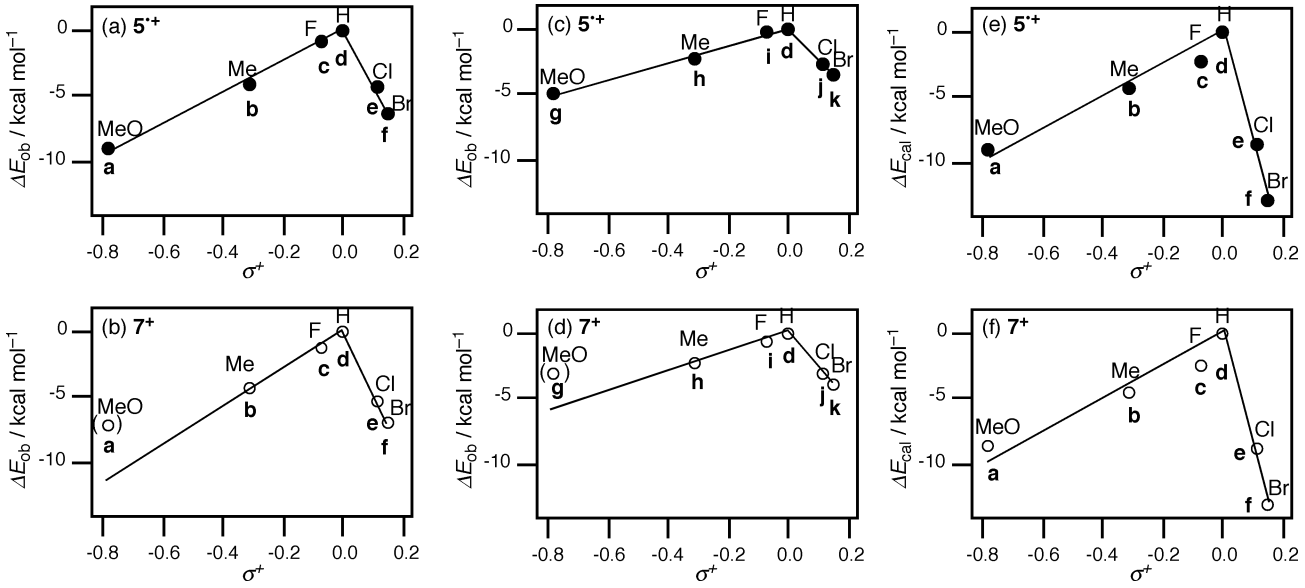

Figure 3. Plots of ΔE_{ob} for the observed electronic absorption energies of (a) **5a**−**f**$^{\bullet+}$, (b) **7a**−**f**$^{+}$, (c) **5g**−**k**$^{\bullet+}$ and **5d**$^{\bullet+}$, and (d) **7g**−**k**$^{+}$ and **7d**$^{+}$ vs σ^{+}, and plots of ΔE_{cal} for the calculated electronic transitions of (e) **5a**−**f**$^{\bullet+}$ and (f) **7a**−**f**$^{+}$ vs σ^{+}.

5a−**f**$^{\bullet+}$ with those of the diarylethyl cations **7a**−**f**$^{+}$. The ρ value ratios, ρ(**5a**−**f**$^{\bullet+}$)/ρ(**7a**−**f**$^{+}$) and ρ'(**5a**−**f**$^{\bullet+}$)/ρ'(**7a**−**f**$^{+}$), obtained from the Hammett plots described above, are found to be 0.87 and 0.89, respectively (Figure 3a−b and eqs 1, 2, 5, and 6). Similarly, the ratios ρ(**5g**−**k**$^{\bullet+}$)/ρ(**7g**−**k**$^{+}$) and ρ'(**5g**−**k**$^{\bullet+}$)/ρ'-(**7g**−**k**$^{+}$), obtained by treatment of data arising from the asymmetrically substituted system, are 0.92 and 0.88, respectively (Figure 3c−d and eqs 3, 4, 7, and 8). The close-to-unity values of these ratios suggest that the substituent effects on E_{ob} for **5**$^{\bullet+}$ are about the same magnitude as that on E_{ob} for **7**$^{+}$. The deviation of ρ(**5**$^{\bullet+}$)/ρ(**7**$^{+}$) and ρ'(**5**$^{\bullet+}$)/ρ'(**7**$^{+}$) from unity might be the result of differences in the conditions (e.g., solvent polarity, temperature) used to perform absorption measurements for **5**$^{\bullet+}$ and **7**$^{+}$. In fact, DFT and TD-DFT calculations strongly indicated that the magnitude of the substituent effects between **5**$^{\bullet+}$ and **7**$^{+}$ were comparable: ρ(**5**$^{\bullet+}$)/ρ(**7**$^{+}$) and ρ'(**5**$^{\bullet+}$)/ρ'(**7**$^{+}$) were about 1 (vide infra). In a manner consistent with a previous interpretation,[10a] it appears that the chromophores in **5**$^{\bullet+}$ undergoing the observed electronic transitions are the same as those in the diarylmethyl cations (subunit I, Scheme 4).

The relative magnitudes of the substituent effects on E_{ob} for the symmetrical and asymmetrical TMM radical cations are seen in the ratios ρ(**5a**−**f**$^{\bullet+}$)/ρ(**5g**−**k**$^{\bullet+}$) and ρ'(**5a**−**f**$^{\bullet+}$)/ρ'(**5g**−**k**$^{\bullet+}$), which have respective values of 1.83 and 1.78. In the diarylethyl cation system, the ratios ρ(**7a**−**f**$^{+}$)/ρ(**7g**−**k**$^{+}$) and ρ'(**7a**−**f**$^{+}$)/ρ'(**7g**−**k**$^{+}$) are 1.93 and 1.76, respectively. The observation that the average ratios are smaller than 2 indicates that the secondary substituent on Ar[2] has less of an effect on the electronic transition energy than the primary substituent on Ar[1]. This conclusion is readily explained by using simple HMO theory, where it can be readily seen that substitution on Ar[1] should more greatly change the energy levels of the parent compounds **5d**$^{\bullet+}$ and **7d**$^{+}$.

DFT Calculations for Evaluating the Substituent Effects. To gain insight into the relationships that may exist between substituent effects and molecular structure, DFT calculations at the (U)B3LYP/cc-pVDZ level were performed for geometry optimization.[11] In Figure 4 is shown the optimized molecular structure of **5d**$^{\bullet+}$. The bond length, *a*, of C-1−C-2 and the dihedral angles, θ and θ', of C-7−C-1−C-2−C-3 and C-7−C-1−C-2−C-5 were optimized to 1.48 Å, 44.0°, and −134.0°, respectively, while similar angles, ω and ω', of C-1−C-2−C-3−C-4 and C-1−C-2−C-5−C-6 were both calculated to be 30.3°. In contrast, the optimized structure of **7d**$^{+}$ has the different ω and ω' values of 23.3° and 31.7°, respectively (Figure 5). As the data in Table 3 suggest, the introduction of substituents has little effect on the optimized structures of **5a**−**f**$^{\bullet+}$ and **7a**−**f**$^{+}$. Importantly, substituents predominantly affect the electronic structure of the TMM radical cations, but they have little if any effect on the molecular structure of these species. Thus, the shifts in the electronic absorption maxima of these radical cations purely reflect electronic effects induced by the substituents.

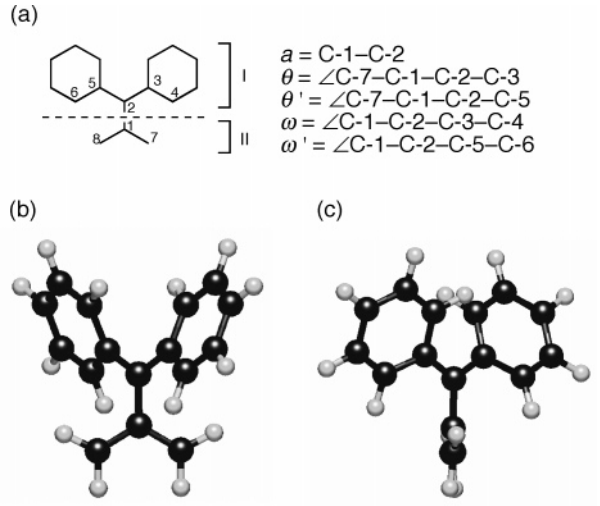

Figure 4. (a) Atom notation and definition of the length (*a*) and dihedral angles (θ, θ', ω, and ω') of **5d**$^{\bullet+}$. The molecular structure of **5d**$^{\bullet+}$ optimized using UB3LYP/cc-pVDZ: (b) front and (c) side views. For details, see ref 11.

TD-DFT calculations were performed on the symmetrical TMM radical cations **5a**−**f**$^{\bullet+}$ and diarylmethyl cations **7a**−**f**$^{+}$ to determine if the observed absorption properties of these species are consistent with their molecular and electronic structures. The electronic transition wavelengths (λ_{cal}) and oscillator strengths (*f*) of **5a**−**f**$^{\bullet+}$ and **7a**−**f**$^{+}$ for optimized structures (vide supra) were calculated by using TD-(U)B3LYP/cc-pVDZ. The data obtained are summarized in Tables 1 and 2. The calculations gave λ_{cal} at 426 nm with $f = 0.68$ for **5a**$^{\bullet+}$,

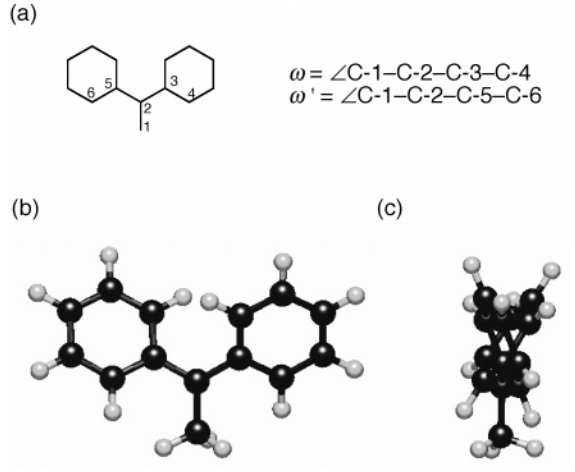

Figure 5. (a) Atom notation and definition of dihedral angles (ω and ω') of **7d**$^+$. The molecular structure of **7d**$^+$ optimized using B3LYP/cc-pVDZ: (b) front and (c) side views.

TABLE 3: Calculated[a] Bond Lengths (*a*) and Dihedral Angles (θ, θ', ω, and ω') of 5a−f$^{\bullet+}$ and 7a−f$^+$

species	*A*/Å	θ/deg	θ'/deg	ω/deg	ω'/deg
5a$^{\bullet+}$	1.49	48.8	−131.2	27.7	27.7
5b$^{\bullet+}$	1.49	45.9	−134.1	29.1	29.1
5c$^{\bullet+}$	1.48	45.6	−134.4	29.3	29.3
5d$^{\bullet+}$	1.48	44.0	−136.0	30.3	30.3
5e$^{\bullet+}$	1.48	45.4	−134.6	29.3	29.3
5f$^{\bullet+}$	1.48	45.5	−134.5	29.3	29.3
7a$^+$				21.5	29.5
7b$^+$				22.5	30.6
7c$^+$				22.6	30.9
7d$^+$				23.3	31.7
7e$^+$				22.5	30.8
7f$^+$				22.4	30.7

[a] Calculations were carried out with (U)B3LYP/cc-pVDZ.

λ_{cal} at 399 nm with $f = 0.62$ for **5b**$^{\bullet+}$, λ_{cal} at 387 nm with $f = 0.51$ for **5c**$^{\bullet+}$, λ_{cal} at 376 nm with $f = 0.44$ for **5d**$^{\bullet+}$, λ_{cal} at 425 nm with $f = 0.67$ for **5e**$^{\bullet+}$, λ_{cal} at 453 nm with $f = 0.70$ for **5f**$^{\bullet+}$, λ_{cal} at 423 nm with $f = 0.77$ for **7a**$^+$, λ_{cal} at 398 nm with $f = 0.70$ for **7b**$^+$, λ_{cal} at 387 nm with $f = 0.33$ for **7c**$^+$, λ_{cal} at 375 nm with $f = 0.52$ for **7d**$^+$, λ_{cal} at 424 nm with $f = 0.76$ for **7e**$^+$, and λ_{cal} at 452 nm with $f = 0.79$ for **7f**$^+$. The calculated λ_{cal} values are systematically shorter than those observed experimentally (λ_{ob}). Plots of the relative calculated transition energies (ΔE_{cal}) vs σ^+, displayed in Figure 3e,f, are nearly linear. The trends match those seen in similar Hammett plots of the experimentally observed transition energies (Figure 3a−b). The lines obtained from plots of the calculated energies of **5a**−**f**$^{\bullet+}$ and **7a**−**f**$^+$ (Figure 3e−f) are shown in eqs 9−12.

$$\sigma^+ < 0$$

$$\Delta E_{cal} = 10.6\sigma^+ - 0.79 \quad \text{for } \mathbf{5a}-\mathbf{f}^{\bullet+} \tag{9}$$

$$\Delta E_{cal} = 10.2\sigma^+ - 0.91 \quad \text{for } \mathbf{7a}-\mathbf{f}^+ \tag{10}$$

$$\sigma^+ > 0$$

$$\Delta E_{cal} = -84.2\sigma^+ + 0.13 \quad \text{for } \mathbf{5a}-\mathbf{f}^{\bullet+} \tag{11}$$

$$\Delta E_{cal} = -85.4\sigma^+ + 0.12 \quad \text{for } \mathbf{7a}-\mathbf{f}^+ \tag{12}$$

Although the ρ values obtained from Hammett treatments of the observed and calculated electronic transition energies are similar in the region $\sigma^+ < 0$, they (ρ') are greatly different (ca.

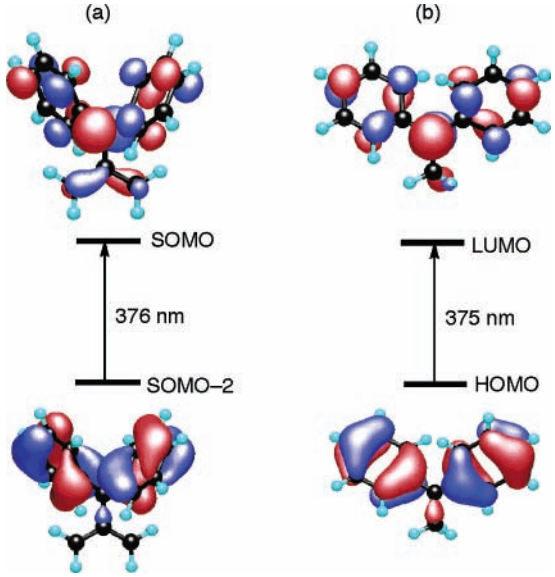

Figure 6. Schematic representation of the MOs of (a) **5d**$^{\bullet+}$ and (b) **7d**$^+$ associated with the calculated electronic transitions. The calculated wavelengths are shown.

two times) in the $\sigma^+ > 0$ region (eqs 1, 2, 5, 6, and 9−12). The ρ(**5a**−**f**$^{\bullet+}$)/ρ(**7a**−**f**$^+$) and ρ'(**5a**−**f**$^{\bullet+}$)/ρ'(**7a**−**f**$^+$) based on the calculated energies are 1.04 and 0.99, respectively (Figure 3e−f and eqs 9−12). Because the ratios are ca. 1, the calculated electronic structure of **5**$^{\bullet+}$ closely resembles that of the localized cation **7**$^+$. As mentioned above, the small deviations from unity seen in ρ(**5**$^{\bullet+}$)/ρ(**7**$^+$) and ρ'(**5**$^{\bullet+}$)/ρ'(**7**$^+$) (Figure 3a−b and eqs 1, 2, 5, and 6) (vide supra) are likely due to differences between the conditions used to record the spectra. Importantly, despite the existence of minor discrepancies the TD-DFT calculation successfully reproduces the observed effects of substituents on E_{ob}.

Analysis of the results obtained from the TD-(U)B3LYP/cc-pVDZ calculations suggests that the electronic transition bands of **5a**−**f**$^{\bullet+}$ and **7a**−**f**$^+$ uniformly originate from the SOMO−X → SOMO ($X = 2$ for **5d**$^{\bullet+}$ and $X = 1$ for **5a**−**c**$^{\bullet+}$ and **5e**−**f**$^{\bullet+}$, respectively) and the HOMO → LUMO transitions, respectively (Figure 6). As is typical for the diphenyl-substituted system (Figure 6), the MOs for the electronic transition band of **5d**$^{\bullet+}$ possess orbital coefficients that are localized mainly in subunit I with a pattern that closely resembles that of **7d**$^+$. This is in accord with the finding that the calculated electronic transition bands of the TMM radical cations **5a**−**f**$^{\bullet+}$ closely correspond to those of the corresponding localized cations **7a**−**f**$^+$.

The TD-(U)B3LYP/cc-pVDZ calculations enable an analysis of the MO origin of the substitutent effects on electronic transition energies of the TMM radical cations **5a**−**f**$^{\bullet+}$ and cations **7a**−**f**$^+$. The Hammett plots show that Cl and Br serve as electron-donating groups in their effects on the energies of electronic transitions. As shown in Figure 7, the changes in the SOMO−X and SOMO energy levels of **5a**−**f**$^{\bullet+}$ that take place upon introducing substituents closely resemble those of the respective HOMOs and LUMOs of **7a**−**f**$^+$. Note that the SOMO−X level of **5e**$^{\bullet+}$ and **5f**$^{\bullet+}$ and the HOMO level of **7e**$^+$ and **7f**$^+$ are higher than the corresponding SOMO−X level of **5d**$^{\bullet+}$ and the HOMO level of **7d**$^+$. This observation strongly suggests that the halogen substituents Cl and Br act as electron-donating groups for the electronic transitions of **5**$^{\bullet+}$ and **7**$^+$. Considering the procedure used to determine σ^+(Scheme 6),[21] this conclusion is seemingly inconsistent with the general

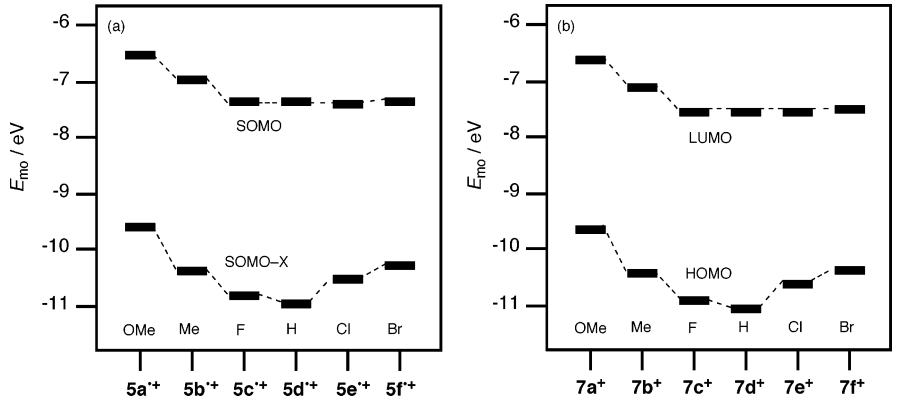

Figure 7. Calculated energy levels of the MOs (E_{mo}) of (a) **5a**−**f**$^{\bullet+}$ and (b) **7a**−**f**$^{+}$ associated with the calculated electronic transition, the SOMO−*X* and SOMO for **5a**−**f**$^{\bullet+}$, and the HOMO and LUMO for **7a**−**f**$^{+}$.

SCHEME 6: Hydrolysis Reaction of the Cumyl Chloride Derivatives (13) Used to Define σ^+

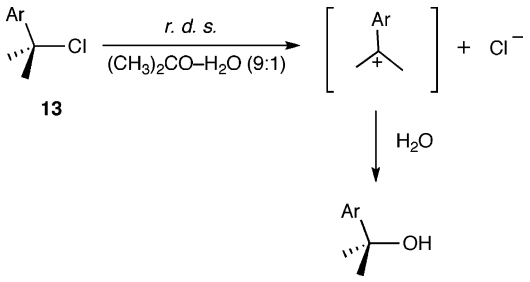

concept that Cl and Br are electron-withdrawing groups in the cationic species. In general, in cations (e.g., cumyl cation), they act as electron-withdrawing groups (by influencing all the MOs) in their contribution to the total energy (Scheme 6). On the other hand, resonance effects dominate substituent effects on the energies of the SOMO and SOMO−*X* levels of **5**$^{\bullet+}$ and the HOMO and LUMO levels of **7**$^{+}$. Consequently, Cl and Br serve as electron-donating groups for the electronic transition of **5**$^{\bullet+}$ and **7**$^{+}$.

It is of interest to compare the effects of the putative electron-donating groups Cl and Br with those of the bona fide electron-donating groups MeO and Me. Although the electron-donating abilities of Cl and Br in cationic species must be weaker than those of MeO and Me, the magnitude of the Cl and Br effects on transition energies of **5**$^{\bullet+}$ and **7**$^{+}$ are of a similar magnitude to those of the MeO and Me (Tables 1 and 2, Figure 3). This seemingly strange behavior can be reasonably explained by inspection of the MOs involved in the electronic transitions. As shown in Figure 7, the strong electron-donating abilities of MeO and Me lead to an increase in the energy of not only the SOMO−*X* of **5**$^{\bullet+}$ and the HOMO of **7**$^{+}$ but also the SOMO of **5**$^{\bullet+}$ and the LUMO of **7**$^{+}$. Conversely, Cl and Br cause increases in the energy levels of the SOMO−*X* of **5**$^{\bullet+}$ and the HOMO of **7**$^{+}$ only compared with those of **5d**$^{\bullet+}$ and **7d**$^{+}$. Therefore, the changes in the SOMO−*X*−SOMO gap of **5**$^{\bullet+}$ and the HOMO−LUMO gap of **7**$^{+}$ induced by a MeO or Me substitution are comparable to those promoted by Cl or Br.

The proposal that the Cl and Br substituents act as electron-donating groups in governing the energies of electronic transition in the TMM radical cations and diarylmethyl cations gains further support from a consideration of calculated partial charge densities (*q*) at the C-2 position (Figures 4 and 5), at which the effects of substituents are most dramatically felt. In Figure 8 is shown the correlation between the relative partial charge densities (Δq) at C-2 in **5a**−**f**$^{\bullet+}$ and **7a**−**f**$^{+}$ vs σ^+. In both

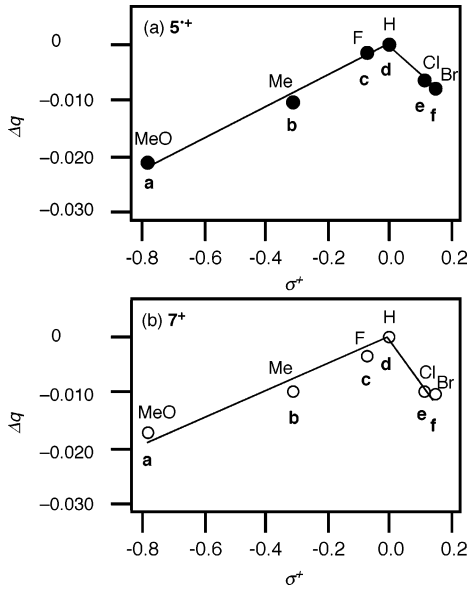

Figure 8. Plots of Δq of (a) **5a**−**f**$^{\bullet+}$ and (b) **7a**−**f**$^{+}$ calculated using (U)B3LYP/cc-pVDZ vs σ^+.

systems, the correlations closely resemble those seen in the ΔE vs σ^+ plots (Figure 3). The lines obtained from these plots forcalculated charge densities at C-2 in **5a**−**f**$^{\bullet+}$ and **7a**−**f**$^{+}$ (Figure 8) are given in eqs 13−16.

$$\sigma^+ < 0$$

$$\Delta q = 0.027\sigma^+ - 0.0002 \qquad \text{for } \mathbf{5a}-\mathbf{f}^{\bullet+} \qquad (13)$$

$$\Delta q = 0.021\sigma^+ - 0.0015 \qquad \text{for } \mathbf{7a}-\mathbf{f}^{+} \qquad (14)$$

$$\sigma^+ > 0$$

$$\Delta q = -0.054\sigma^+ - 0.0001 \qquad \text{for } \mathbf{5a}-\mathbf{f}^{\bullet+} \qquad (15)$$

$$\Delta q = -0.074\sigma^+ + 0.0003 \qquad \text{for } \mathbf{7a}-\mathbf{f}^{+} \qquad (16)$$

The ρ and ρ' values obtained from Hammett treatments of the calculated charge densities in **5a**−**f**$^{\bullet+}$ are similar to those found for the respective calculated values in **7a**−**f**$^{+}$. These results suggest that substituents affect the **5**$^{\bullet+}$ and **7**$^{+}$ contain the same diarylmethyl cation chromophore. Importantly, the introduction of Cl and Br groups induces an incremental increase in the negative charge densities at C-2 (Figure 8). This suggests that Cl and Br groups act as electron-donating groups in the same manner as do MeO or Me groups. In this manner, the correlation

of ΔE vs σ^+ with the boundary point at $\sigma^+ = 0.00$ (Figure 3) is associated with red-shifts of the absorption bands caused by the electron-donating ability of Cl and Br.

Conclusion

In this effort, we have explored the effects of aryl-ring substituents on the energies of electronic transitions (E) of the TMM radical cations **5a**−**k**$^{\bullet+}$ and the diarylmethyl cations **7a**−**k**$^+$ by using electronic absorption spectroscopy and DFT calculations. By comparing the Hammett plots of ΔE_{ob} and ΔE_{cal} data, we found that **5**$^{\bullet+}$ has a considerably localized electronic structure containing a diarylmethyl cation chromophore (subunit I). The results of the DFT calculation indicate that the molecular and electronic structures of **5**$^{\bullet+}$ are highly twisted and contain a substantially localized electronic state, in which the positive charge and spin are localized in the respective subunit I and subunit II. Although the twisted structure of **5**$^{\bullet+}$ is in line with the distorted structure of the parent radical cation **1**$^{\bullet+}$, but the causes of this conformational distortion are different: the **5**$^{\bullet+}$ twisting is caused by steric interactions between the aryl and allyl moieties,[8,10a] whereas **1**$^{\bullet+}$ the distortion is a result of electronic interactions.[15]

The similarity in the electronic absorption bands of **5a**−**k**$^{\bullet+}$ and **7a**−**k**$^+$ is due to the presence of comparable SOMO−X → SOMO and HOMO → LUMO transitions. In this sense, the substituent effects in **5a**−**k**$^{\bullet+}$ and **7a**−**k**$^+$ on E correspond in a systematic manner. We showed that, in these systems, a secondary substituent on Ar^2 is less influential than a primary substituent on Ar^1. These results provide important basic information about TMM derivatives, and they offer insight into the precise molecular structure of these species needed for practical applications such as to the design of organic light-emitting diodes using an open-shell biradical **5**$^{\bullet\bullet}$.[13] Furthermore, the results of this effort show that Cl and Br act as electron-donating groups in influencing electronic transitions of cationic species.[22] This finding is seemingly counter to the common knowledge that Cl and Br are electron-withdrawing groups with $\sigma^+ > 0$. Further studies aimed at support for this conclusion are now in progress.

Acknowledgment. H. I. and K. M. gratefully acknowledge financial support from Grants-in-Aid for Scientific Research on Priority Areas (nos. 14050008 and 17029058 in area no. 417) and others (nos. 16655018, 18037063, and 19350025) from the Ministry of Education, Culture, Sports, Science, and Technology of Japan. H. I. gratefully acknowledges the Shorai Foundation, the Iketani Foundation, and the Mazda Foundations for Science and Technology. We also thank Professors M. Ueda (TU), T. Okuyama (University of Hyogo), M. Mishima (Kyushu University), and K. Nakata (Hosei University) for their valuable discussions.

Supporting Information Available: The general method of the experiments, physical data for key compounds, electronic transition spectra of **5a**−**c**$^{\bullet+}$, **5e**−**k**$^{\bullet+}$, **7a**−**c**$^+$, and **7e**−**k**$^+$, and DFT calculation results for **5a**−**f**$^{\bullet+}$ and **7a**−**f**$^+$ optimized using DFT calculations. This material is available free of charge via the Internet at http://pubs.acs.org.

References and Notes

(1) Moffitt, W. E. In Coulson, C. A. *J. Chim. Phys. Physicochim. Biol.* **1948**, *45*, 243−248.

(2) Dowd, P. *J. Am. Chem. Soc.* **1966**, *88*, 2587−2589.

(3) (a) Trost, B. M. *Angew. Chem., Int. Ed. Engl.* **1986**, *25*, 1−20. (b) Allan, A. K.; Carroll, G. L.; Little, R. D. *Eur. J. Org. Chem.* **1998**, 1−12. (c) Little, R. D. *Chem. Rev.* **1996**, *96*, 93−114. (d) Maiti, A.; Gerken, J. B.; Masjedizadeh, M. R.; Mimieux, Y. S.; Little, R. D. *J. Org. Chem.* **2004**, *69*, 8574−8582.

(4) Bregant, T. M.; Groppe, J.; Little, R. D. *J. Am. Chem. Soc.* **1994**, *116*, 3635−3636.

(5) (a) Dougherty, D. A. *Acc. Chem. Res.* **1991**, *24*, 88−94. (b) Matsumoto, T.; Ishida, T.; Koga, N.; Iwamura, H. *J. Am. Chem. Soc.* **1992**, *114*, 9952−9959. (c) Jacobs, S. J.; Shultz, D. A.; Jain, R.; Novak, J.; Dougherty, D. A. *J. Am. Chem. Soc.* **1993**, *115*, 1744−1753.

(6) (a) Roth, W. R.; Winzer, M.; Lennartz, H. W.; Boese, R. *Chem. Ber.* **1993**, *126*, 2717−2725. (b) Abe, M.; Adam, W. *J. Chem. Soc., Perkin Trans. 2* **1998**, 1063−1068. (c) Roth, W. R.; Wildt, H.; Schlemenat, A. *Eur. J. Org. Chem.* **2001**, 4081−4099.

(7) (a) Berson, J. A.; Corwin, L. R.; Davis, J. H. *J. Am. Chem. Soc.* **1974**, *96*, 6117−6179. (b) Crawford, R. J.; Tokunaga, H.; Schrijver, L. M. H. C.; Godard, J. C. *Can. J. Chem.* **1978**, *56*, 998−1004. (c) Cichra, D. A.; Duncan, C. D.; Berson, J. A. *J. Am. Chem. Soc.* **1980**, *102*, 6527−6533. Roth, W. R.; Winzer, M.; Lennartz, H. W.; Boese, R. *Chem. Ber.* **1993**, *126*, 2717−2725. (b) Abe, M.; Adam, W. *J. Chem. Soc., Perkin Trans. 2* **1998**, 1063−1068. (c) Roth, W. R.; Wildt, H.; Schlemenat, A. *Eur. J. Org. Chem.* **2001**, 4081−4099. (d) Miyashi, T.; Ikeda, H.; Takahashi, Y.; Akiyama, K. In *Advances in Electron Transfer Chemistry*; Mariano, P. S., Ed.; JAI: London, 1999; Vol. 6, pp 1−39.

(8) Ikeda, H.; Namai, H.; Taki, H.; Miyashi, T. *J. Org. Chem.* **2005**, *70*, 3806−3813.

(9) See also; Turro, N. J.; Mirbach, M. J.; Harrit, N.; Berson, J. A.; Platz, M. S. *J. Am. Chem. Soc.* **1978**, *100*, 7653−7658.

(10) (a) Ikeda, H.; Akiyama, K.; Takahashi, Y.; Nakamura, T.; Ishizaki, S.; Shiratori, Y.; Ohaku, H.; Goodman, J. L.; Houmam, A.; Wayner, D. D. M.; Tero-Kubota, S.; Miyashi, T. *J. Am. Chem. Soc.* **2003**, *125*, 9147−9157. (b) Ikeda, H.; Nakamura, T.; Miyashi, T.; Goodman, J. L.; Akiyama, K.; Tero-Kubota, S.; Houmam, A.; Wayner, D. D. M. *J. Am. Chem. Soc.* **1998**, *120*, 5832−5833. (c) Miyashi, T.; Takahashi, Y.; Mukai, T.; Roth, H. D.; Schilling, M. L. M. *J. Am. Chem. Soc.* **1985**, *107*, 1079−1080.

(11) Ikeda, H.; Namai, H.; Kato, N.; Ikeda, T. *Tetrahedron Lett.* **2006**, *47*, 1857−1860.

(12) Namai, H.; Ikeda, H.; Mizuno, K. Unpublished result.

(13) Namai, H.; Ikeda, H.; Hoshi, Y.; Kato, N.; Morishita, Y.; Mizuno, K. **2007**, To be submitted.

(14) Ikeda, H.; Namai, H.; Kato, N.; Ikeda, T. *Tetrahedron Lett.* **2006**, *47*, 1501−1504.

(15) Komaguchi, K.; Shiotani, M.; Lund, A. *Chem. Phys. Lett.* **1997**, *265*, 217−223.

(16) Becke, A. D. *J. Chem. Phys.* **1993**, *98*, 5648−5652.

(17) Lee, C.; Yang, W.; Parr, R. G. *Phys. Rev. B.* **1988**, *37*, 785−789.

(18) Frisch, M. J.; Trucks, G. W.; Schlegel, H. B.; Scuseria, G. E.; Robb, M. A.; Cheeseman, J. R.; Zakrzewski, V. G.; Montgomery, J. A., Jr.; Stratmann, R. E.; Burant, J. C.; Dapprich, S.; Millam, J. M.; Daniels, A. D.; Kudin, K. N.; Strain, M. C.; Farkas, O.; Tomasi, J.; Barone, V.; Cossi, M.; Cammi, R.; Mennucci, B.; Pomelli, C.; Adamo, C.; Clifford, S.; Ochterski, J.; Petersson, G. A.; Ayala, P. Y.; Cui, Q.; Morokuma, K.; Malick, D. K.; Rabuck, A. D.; Raghavachari, K.; Foresman, J. B.; Cioslowski, J.; Ortiz, J. V.; Stefanov, B. B.; Liu, G.; Liashenko, A.; Piskorz, P.; Komaromi, I.; Gomperts, R.; Martin, R. L.; Fox, D. J.; Keith, T.; Al-Laham, M. A.; Peng, C. Y.; Nanayakkara, A.; Gonzalez, C.; Challacombe, M.; Gill, P. M. W.; Johnson, B. G.; Chen, W.; Wong, M. W.; Andres, J. L.; Head-Gordon, M.; Replogle, E. S.; Pople, J. A. *Gaussian 98*, revision A.11.4; Gaussian, Inc.: Pittsburgh, PA, 1998.

(19) *WinMOPAC 3.9*; Fujitsu Ltd.: Tokyo, Japan, 2004.

(20) The data for **7a**$^+$ and **7g**$^+$ were excluded from the least squares method calculation because these data deviated significantly from the lines obtained for the data for **7b**−**d**$^+$ and **7h**$^+$, **7i**$^+$, and **7d**$^+$. This is thought to be due to protonation at the MeO groups in FSO_3H.

(21) (a) Brown, H. C.; Okamoto, Y. *J. Am. Chem. Soc.* **1958**, *80*, 4979−4987. (b) Brown, H. C.; Okamoto, Y. *J. Am. Chem. Soc.* **1957**, *79*, 1913−1917.

(22) As an alternative explanation for the two-phase linear free energy relationships, one of the reviewers suggested that Cl and Br groups might be due to heavy atom effects that cause a normally forbidden, low energy transition to become allowed. Typically, the heavy atom effects alter transition probability for state-to-state transition involving multiplicity changes. However, the SOMO−X−SOMO transition of **5**$^{\bullet+}$ occurs conserving a doublet multiplicity, although the HOMO−LUMO transition of **7**$^+$ may involve multiplicity changes. The fact that similar two-phase liner free energy relationships were observed for both **5**$^{\bullet+}$ and **7**$^+$ imply that the heavy atom effects on the transition energy in this system are not likely. In addition, DFT calculation afforded similar f (> 0.3) of the transition interested for all of **5**$^{\bullet+}$. This is also in line with our conclusion.